Dynamic Fracture Analysis for Shale Material by Peridynamic Modelling

Zhanqi Cheng[1], Zhenyu Wang[1] and Zhongtao Luo[2, *]

Abstract: In this work, a bond-based peridynamics (PD) model was built to analyze the dynamic fracture of shale material. Both the the convergence studies and the result of dynamic crack propagation were presented. As well-known, crack propagation, aggregation, and bifurcation play an critical role in the failure analysis of brittle materials such as shale. The dynamic crack propagation and branching analysis of shale by using the PD method were discussed. Firstly, the valid and accuracy of the PD model for the rock materials was verified by comparing with the existed numerical results. Secondly, we discussed the convergence both with uniform grid refinement (*m*-convergence) and decreasing the peridynamics horizon (δ-convergence). Then the shale material with two pre-crack under uniaxial compression using the present PD model were discussed, and the influence of the different angle of flaws on the behavior of crack propagation was also analyzed. The results shows that both the loading conditions and the angle of flaws can influences the crack propagation in shale.

Keywords: Peridynamics, shale, dynamic fracture, crack propagation, dynamic loads.

1 Introduction

As the heterogeneous and brittle material in nature, the crack propagation pattern and the interaction of the cracks play the key role in dynamic failure of rocks [Ravi-Chandar and Knauss (1984a, b); Zhou, Wang and Qian (2016)]. Especially under dynamic loading, the transient release of energy leads to stress re-distribution, which leads a sharp decline in rock mechanical properties and rapid crack propagation [Yang, Tang and Xia (2012)]. There are many joints in rock media, which appear in bunchings and have similar orientation and mechanical properties. It can be found that the discontinuities can be any scale can exist in the grain boundaries, joint and regional faults, which significantly reduces the stiffness and strength of rocks. Hence, investigation of the crack initiation, curving and bifurcation in rock medium are both beneficial to comprehend the failure of rock material and very important for practical applications of rock engineering.

Just as well known, because cracks, joints and faults in rock materials dominate the failure process of rock materials, the simulation of dynamic fracture mechanicsm in rock

---

[1] School of Civil Engineering, Zhengzhou University, Zhengzhou, 450001, China.

[2] School of Material Science and Engineering, Zhengzhou University, Zhengzhou, 450001, China.

[*] Corresponding Author: Zhongtao Luo. Email: luozhongtao@126.com.

materials is a difficult challenge for computational mechanics mass. In recent decades, in addition to accurately obtaining the dynamic fracture behavior of rock materials, researchers in computational mechanics have developed many methods to research the dynamic crack propagation of rock materials [Wang and Shrive (1993); Rannou, Limodin and Rthore (2010); Li and Wong (2012); Zhou, Bi and Qian (2016)]. The numerical manifold method was used by Wong et al. [Wong and Wu (2014)] to study the gradual failure in rock. They used a continuous and discontinuous combined method to conduct analysis synthesis. By using the finite difference method, a numerical model considering both material inhomogeneity and micro-defects at element scale is established by Li et al. [Li, Konietzky and Li (2016)]. Their numerical results are in well accordance with the physical observation of fracturing process in brittle rocks. For obtaining the fracture process of rock materials, a numerical method is developed to reproduce the transition from continuum to discontinuity [Cai (2013)]. A multi-scale numerical modle was explored to study the fracture behavior of porous polygranular graphite subject to neutron damage and radiolylic oxidation, in which the relationship between the amount of microstructure of material and the crack propagation were considered [Smith, Schlangen, Flewitt et al. (2016)]. It should be noted that most numerical methods are now developed by modifying the traditional finite element method (FEM). The governing equations of these methods are partial differential equations based on classical continuum mechanics. When analyzing discontinuous problems such as cracks, the crack surface must be defined the new boundary in the renewal domain, which requires special modeling methods (such as adaptive mesh reconstruction). To find a way ot of the problem, a representative extended finite element method (XFEM), which does not require remeshing elements, is proposed to investigate crack propagation [Belytschko and Black (1999); Song, Wang and Belytschko (2008); Xu, Liu, Liu et al. (2014)]. It describes the problem of discontinuous mechanics by introducing additional functions that can reflect discontinuities into finite element functions, but XFEM is still challenged in the face of complex crack behavior, such as 3D fracture problems, multi-scale cracks, crack branching and curving and so on.

To overcome the discontinuitiy problem of displacement field in fracture problem, several kinds of mesh-free methods were built such as Smooth Particle Hydrodynamics (SPH) [Charkrabory and Shaw (2013); Raymond, Lemiale, Ibrahim et al. (2014)], Material Point Mehod (MPM) [Pandolfi (2013)], Element-free Galerkin method (EFGM) [Zi, Rabczuk and Wall (2007)] and so on. In these continuum-type methods, special standards are required to determine when to bifurate a dynamic crack and to demonstrate the crack propagation pattern [Ha and Bobaru (2011); Song, Wang and Belytschko (2008)]. As a numerical method, molecular dynamics (MD) was conducted to model and investigate the dynamic fracture problem of brittle materials [Abraham (2005); Nakano, Kalia and Vashista (1995)]. However, there are huge amounts of the molecular elements to be used to model the macro fracture for materials. Thus, MD is only used to analyze the crack initiation and propagation in brittle materials.

Alternatively, to ease inadequacies of local continuum theory, peridynamics (PD) has been proposed to model the problem of discontinuities, especial the problem of dynamic failure [Silling (2000); Silling and Askari (2005); Silling, Epton, Weckner et al. (2007)]. Essentialy, PD is an integral nonlocal reconstruction for differential control equations in

the continuum mechanics. This means that the discontinuity in the PD model no longer defines the displacement derivatives used in classical mechanics equations. Thus, PD can model the crack initiation and propagation without and special techniques. PD have two versions, the original formulation is bond-based, and the advanced version is state-based. However, the bond-based PD has a restriction that is the poisson's ratio is 1/3 in plane stress state and 1/4 in 3D and plane strain state. The state-based PD is more general, where the bond interaction between points is determined by deformations of points of the entire family. Agwai et al. [Agwai, Guven and Madenci (2011)] studied the fidelity of PD theory in forcasting crack propagation through the comparative research. For multi-crack dynamic fracture problems involving complex branched joints, PD theory is considered as a suitable analytical method. By using the state-based model, the analysis of the damage growth in biomaterial specimen under thermomechanical loading is carried out by Zhang et al. [Zhang and Qiao (2018)] carried the analysis for the prediction result of of bimaterial structures under by state-based PD model. Ha et al. [Ha and Bobaru (2011)] investigated the dynamic fracture in brittle composite materials by using PD. Ren et al. [Rabczuk and Ren (2017)] provided a double-horizon PD model to simulate dynamic brittle fracture problems. Fan et al. [Fan and Li (2017)] showed the result about soil breakage under buried blasting loads. Fan et al. [Fan, Guy and Li (2015)] simulate the soil fragmentation caused by the explosion of buried explosives based on state-based peridynamics and shown the numeriacl results are agreement with the experiment. By using the PD, Gu et al. [Gu, Zhang , Huang et al. (2016)] analyzed the elastic wave spread, crack propagation, and shock fracture of concrete Brazilian discs in SPHB tests. Cheng et al. [Cheng, Zhang,Wang et al. (2015); Cheng, Liu, Zhao et al. (2018)] conducted a study about the dynamic crack propogation in FGMs.

For the rock-like material, some researchers have investigated its dynamic fracture behavior. Zhou et al. [Zhou, Wang and Qian (2016)] studied the crack propagation patterns in rock-like materials under dynamic loads based on the extended non-ordinary state-based PD. Wang et al. [Wang, Zhou and Xu (2016); Wang, Zhou and Shou (2017); Wang, Zhou, Wang et al. (2018)] conducted several PD analysis for tracking of crackpropagation in rock and brittle materials. Ni et al. [Ni, Zhu, Zhao et al. (2018)] used the irregular finite element mesh in PD model to analyze the   crack problem in quasi brittle materials using. Lai et al. [Lai, Ren, Fan et al. (2015)] constrcuted the nonlinear peridynamics model of drainage and statueated geomaterials and used to simulate dynamic fracture casued by impact loads. However, the solutions to deal with the crack initiation, propagation and coalescence in layered rock materials under dynamic loads are also limited.

In this work, the bond-based PD model are employed to simulate and investigate the shale with bedding structure subjected dynamic loading. According to the elastic and fracture characteristics of the precise positions of these nodes in rock materials, a PD model for heterogeneous rock materials is constructed by using the parallel bonds between the two nodes. To study the dynamic fracture problems, the rock plates with one or several cracks are modeled under dynamic loading. The effect of material properties, time and size of dynamic loading on dynamic failure behavior are studied in the field of crack ways geometry and crack growth rate.

The organization of the paper is as follows. We briefly introduce the PD method in Section 2 and describe the bond parameters in layered rock in Section 3. In Section 4, we first conducted a study of the m-convergence and δ-convergence and provide the verification of the present model, then under the dynamic loads, we study the crack propagation pattern and the interaction of the cracks. Further, the conclusions are given in Section 5.

2 Brief review of bond-based peridynamic formulation

In the bond-based PD theory, the governing equations are provided by:

$$\rho \ddot{u}(x,t) = \int_{H_x} f\left(u(x,t) - u(x,t), x' - x'\right) dV_{x'} + b(x,t) \tag{1}$$

where f is the pairwise force function in the PD bond that connects point x' to x, u is the displacement vector field, $b(x,t)$ is the body force density field, ρ is mass density in the reference configuration and the H_x is a neighborhood of x called the "horizon region". Its radius is called the horizon and is denoted by δ, as shown in Fig. 1, $\{x' \in R : \|x' - x\| \leq \delta\}$.
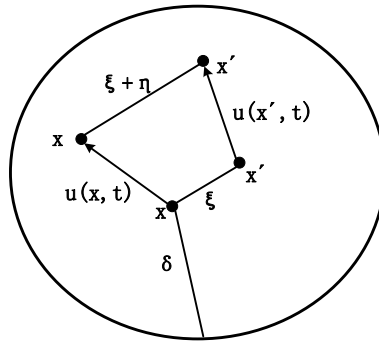
Figure 1: Illustration of peridynamic variables
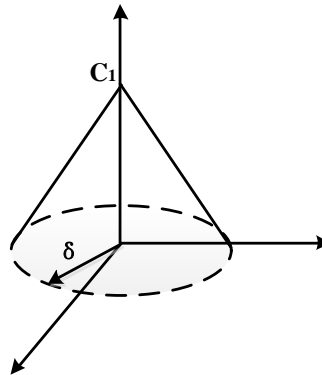
Figure 2: Conical micro-modulus functions

For a micro-elastic material, the pairing force is determined by the micro-potential function ω [Silling (2000)]:

$$f(\eta,\xi) = \frac{\partial \omega}{\partial \eta}(\eta,\xi) \tag{2}$$

where $\xi = x' - x$ and $\eta = u' - u$ is the relative position vector and relative displacement vector, respectively, as is shown in Fig. 1. When the magnitude of the force is linearly relation to the relative elongation, the following micro-potential function can be achived as:

$$\omega(\eta,\xi) = \frac{c(\xi)s^2\xi}{2} \tag{3}$$

where $\xi = \|\xi\|$ and $s = \frac{\|\eta + \xi\| - \|\xi\|}{\|\xi\|}$ is the relative bond stretch. $c(\xi)$ is the micro-modulus function, which describes the elastic stiffness of a bond. Corresponding to a linear micro-elastic potential, the pairing force has the following form:

$$f(\eta,\xi) = \begin{cases} \dfrac{\xi + \eta}{\|\xi + \eta\|}c(\xi)s \quad , \quad \xi \leq \delta \\ 0 \qquad\qquad\quad , \quad \xi > \delta \end{cases} \tag{4}$$

Here, we can notice that inside the horizon region ($\xi \leq \delta$), the pairwise force between the material points x' and x, when $\xi > \delta$, the material points x' and x do not have the pairwise force. In this paper, the conical micro-modulus function for plane stress state is used, and the its form is [Ha and Bobaru (2011)]:

$$c(\xi) = c_I\left(1 - \frac{\xi}{\delta}\right) = \frac{24E}{\pi\delta^3(1-\upsilon)}\left(1 - \frac{\xi}{\delta}\right) \tag{5}$$

The conical micro-modulus function is showted in Fig. 2. In the bond-based PD, a particle interacts with any particle inside its horizon only through a central potential. This assumption leads to an effective Poisson's ratio of 1/3 in 2D and 1/4 in 3D.

For the sake of leading failure into the PD model, we introduced a "critical relative elongation", defined as s_0. we define that the bonds will broken when their elongations exceed s_0. In plane problem, the energy of unit fracture length, which completely separates an body into two halves, is called fracture energy G_0. If we let the fracture energy G_0 equal to the work done in PD material, G_0 in the plane stress state is obtained as:

$$G_0 = 2\int_0^\delta \int_z^\delta \int_0^{cos^{-1}(\frac{z}{\xi})} \left[\frac{c(\xi)s_0^2 \xi}{2} \right] \xi \mathrm{d}\theta \mathrm{d}\xi \mathrm{d}z \qquad (6)$$

Substituting Eq. (5) into Eq. (6), the critical relative elongation s_0 for the conical micro-modulus function in 2D is:

$$s_0 = \sqrt{\frac{5\pi G_0}{9E\delta}} \qquad (7)$$

It can be seen that s_0 is determined by the material properties and the horizon δ.

3 The peridynamic model of shales

As we know, there are many natural tiny cracks in the rock, under the action of the load, the cracks will increase, the effective stress of the rock micro-bodies will also continue to rise, resulting in new defects continue to eventually lead to the overall decline in rock strength. Under continuous loading, we can assume that the rock micro-bodies behave macroscopically as isotropic. In addition, for shale, the bedding structure is common, so the difference of the material properties in the ply should be considered. As is shown in Fig. 3, the bond of the material is classification into two terms, the inner-layer bond and the inter-layer bond.

| Layer I |
| Layer II |
| Layer IЩ |
| Layer VI |
| ⋮ |
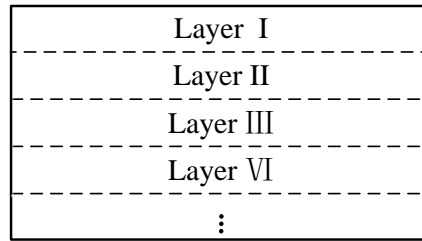
Figure 3: Shale material with bedding structure

3.1 The inner-layer bond

According to the PD model, any point i has its family points, whcin the distance between point i and them is shorter than the horizon size δ. The bonds exist between the material point i and its family points. If both point i and all its family points are in the same layer, all the bonds between point i and its family points are called the inner-layer bond. The inner-layer bond is shown in Fig. 4. The micro-modulus functions $c(\xi)$ and the critical strain s_0 can be obtained by using Eq. (5) and Eq. (7).

3.2 The interlayer bond

It can be noticed from Fig. 5(a) that the material point i has its family points j, k, f, n, m, e, l, h.points i, j, k, f, n, m are located in the same ply as point i,
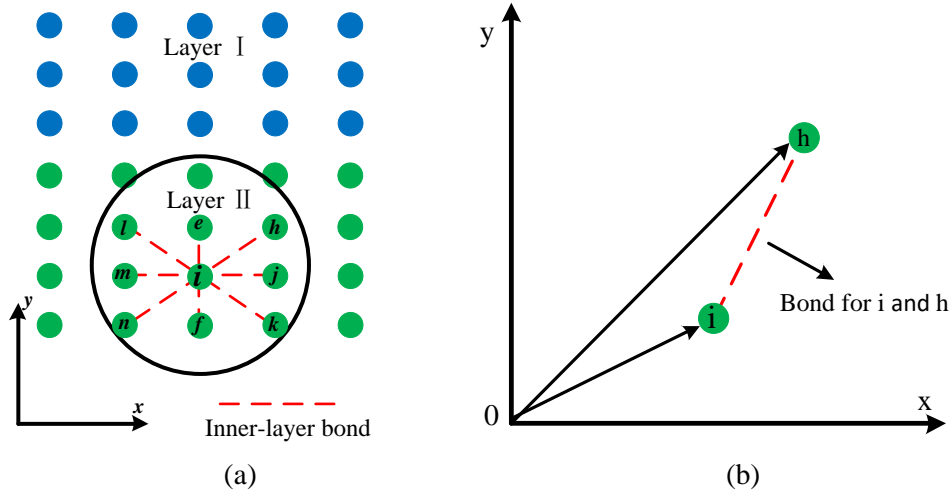
and the bonds between material point i and j, k, f, n, m are the inner-layer bonds. On the contrary, the material points e, l, h do notlocate in the same layer as point i. For the material properties in different layer is different, the bonds between points e, l, h and point i is called inter-layer bonds. Cheng et al. [Cheng, Liu, Zhao et al. (2018)] have introduced the two parallel bonds to simulate FGM. We will also use the two parallel bonds to adapt the inter-layer bonds between two points with different mechanical properties. E_i, ρ_i, G_{0i} and E_h, ρ_h, G_{0h} are the Young's modulus, density, and fracture energy of points i and h, respectively. The two parallel bonds connect the two points are shown in Fig. 5(b). Therefore, for the concial micromodulus function, Eq. (5) and Eq. (7) can be rewrite as:

$$c_i(\xi) = c_I\left(1 - \frac{\xi}{\delta}\right) = \frac{12E_i}{\pi\delta^3(1-v)}\left(1 - \frac{\xi}{\delta}\right) \tag{8a}$$

$$c_h(\xi) = c_I\left(1 - \frac{\xi}{\delta}\right) = \frac{12E_h}{\pi\delta^3(1-v)}\left(1 - \frac{\xi}{\delta}\right) \tag{8b}$$

$$s_{0i} = \sqrt{\frac{5\pi G_{0i}}{9E_i\delta}} \; ; \quad s_{0h} = \sqrt{\frac{5\pi G_{0h}}{9E_h\delta}} \tag{9}$$

Terms $c_i(\xi)$, s_{0i} and $c_h(\xi)$, s_{0h} are represent the micro-modulus function and critical relative elongation of two bonds between i and h, respectively. Here, we must point out that the two bonds will break at the same time [Cheng, Liu, Zhao et al. (2018)].


(a)   (b)

Figure 4: Classification of PD bonds in layered shale: (a) inner-layer bond; (b) the inner-layer bond between material point i and h in one layer
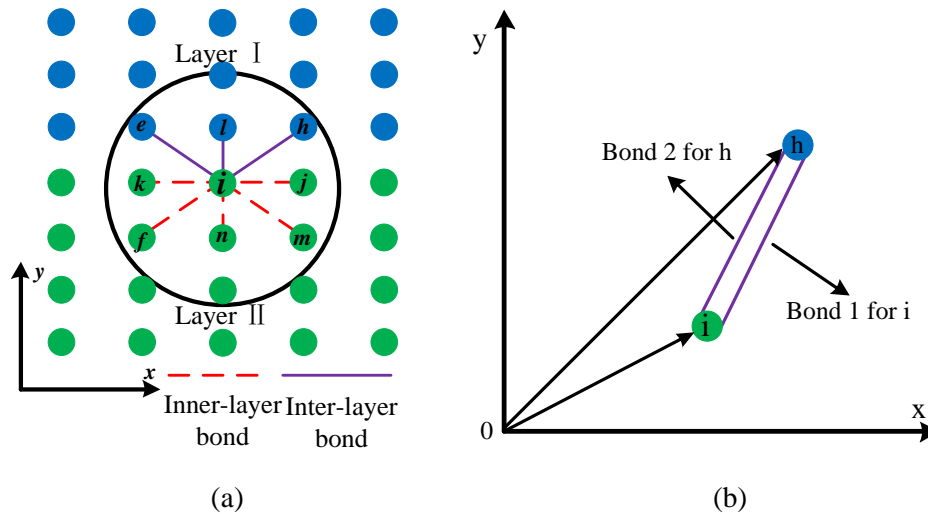
Figure 5: Classification of PD bonds in layered shale: (a) inter-layer bond; (b) the inter-layer bond between material point *i* and *h* in one layer

4 Numerical result and convergence studies

In this section, the materials specimans from the Longmaxi Formation shale of the Changxin well $1^{\#}$ in the southern Sichuan Basin were chosen [Wang, Dong, Li et al. (2012)]. Due to its moderate mechanical properties, high elastic modulus, brittle and hard texture, the chosen shale material is easier to form natural fractures and facilitate artificial prefabricated fractures. At the same time, the types of pores in shale are abundant, with a large number of natural micro-cracks, which is very suitable for studying the cracks and expansion in rock.
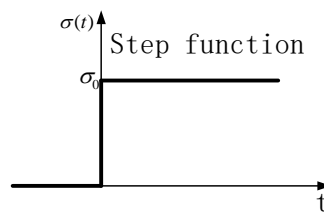
Figure 6: The vurve of load

4.1 Convergence studies of in dynamic crack propagation in shales

The PD model has been proved to be valid in the dynamic crack problem of shale material [Wang, Zhou and Xu (2016); Zhou, Wang and Qian (2016)]. In this part, the convergence of the present model is conducted by studying a edge crack in shale sample under tensile stress.

Table 1: Mechanical parameters of shale specimens [Wang, Dong and Li et al. (2012)]

E (GPa)	K_{IC} (MPa·m$^{1/2}$)	ρ(kg/m^3)
8.58	0.99	2550

4.1.1 Problem setup

In order to study the numerical convergence for PD model, an   plate with a pre-notch with length of 50 mm is investigated under symmetrically dynamic tension loads on the boundary, the dimensions of the plate is 100 mm×40 mm, as shown in Fig. 7. The shale material used in this study is Longmaxi Formation shale from Sichuan, China [Wang, Dong, Li et al. (2012)] and the investigated shale specimen's mechanical properties are listed in Tab. 1. Ravi-Chander et al. [Ravi-Chander and Knauss (1984)] had analyzed this structure of homogeneous material through experiment. $\sigma(t)$ is the dynamic tensile load, as shown in Fig. 6. Beyond the loads symmetrically imposed on the boundary of the slate board, no other boundary conditions are specified.
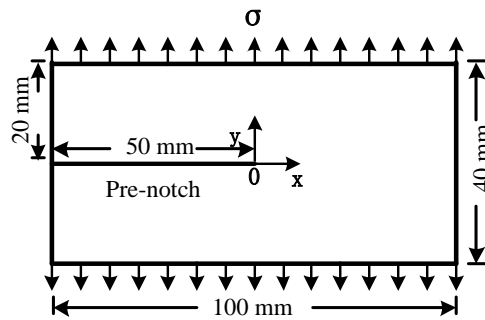

Figure 7: Specimen geometry and boundary conditions

4.1.2 Numerical convergence

The convergence of PD model for dynamic brittle fracture has been studied be Bobaru el al. [Bobaru, Yang, Alves et al. (2009)]. In this model, we discuss two numerical convergence criteria: *m*-convergence and *δ*-convergence. In this section, The convergence is conducted through the crack propagation.

For the *δ*-convergence, we studied *m*=4 and the horizon size is 2 mm, 1.6 mm, and 1.33 mm, respectively. Under the term of the pre-crack along the *x* direction and σ₀=8.5 MPa for PD model for the convergence study. The grid spacing determines by the each horizon size because of *m* is unchanged, hence, the grid spacing Δ*x* values are 0.5 mm, 0.4 mm, and 0.33 mm, respectively. As is shown in Fig. 8, we provide the result for the PD simulations above 60 μs. It can be observed from the result that as the horizon lessens, the crack basically remain unchanged, but become clearer. It is also in agreement with the affirmation that the damage diffusion is affected by the size of horizon.

(a) m=4, Δx=0.5 mm
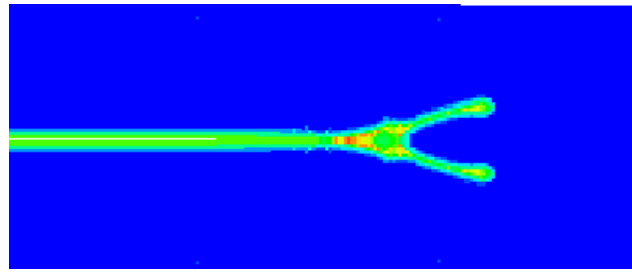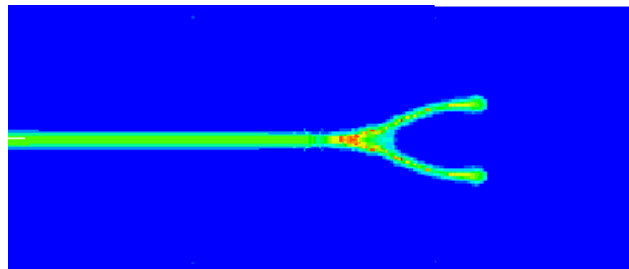
(b) m=4, Δx=0.4 mm
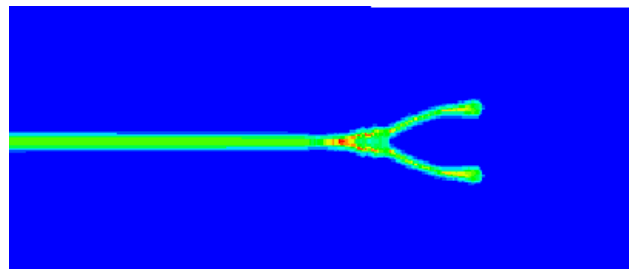
(c) m=4, $\Delta x = 0.33$ mm

Figure 8: Crack propagation and brabching with different δ; the damage maps shown are at 60 μs

For the *m*-convergence study, the model and the load condition are similar with the δ-convergence, we conducted the study with fixed horizon size: δ=2 mm. We performed Δ*x*=0.8 mm (m=2.5), Δ*x*=0.5 mm (m=4) and Δ*x*=0.4 mm (m=5). It can be observed from Fig. 9 that the crack path at 60 μs simulated by PD when the number of nodes in the horizon is large enough (*m*>4), the cracks did not change further. Furthermore, the lengths of crack propagation in Fig. 8(b) is very close to Fig. 8(c). This indicates that the crack velocity was very close to each other in the two cases. For better balance the computation cost and accuracy, we selected the horizon size δ=2 mm and *m*=4.

(a) m=2.5, Δx=0.8 mm


(b) m=4, Δx=0.5 mm
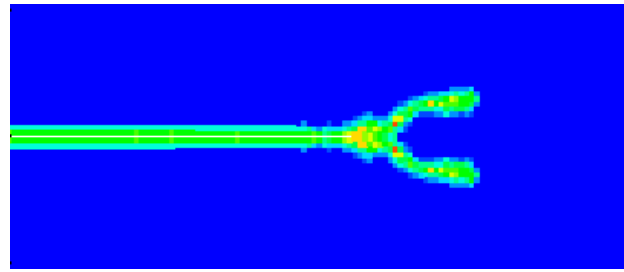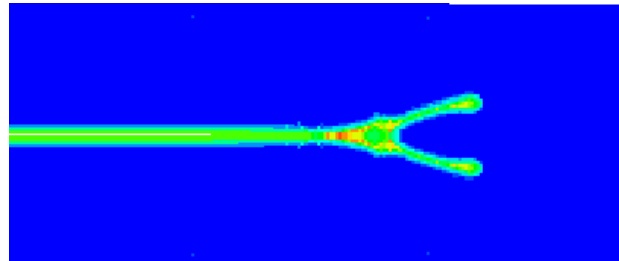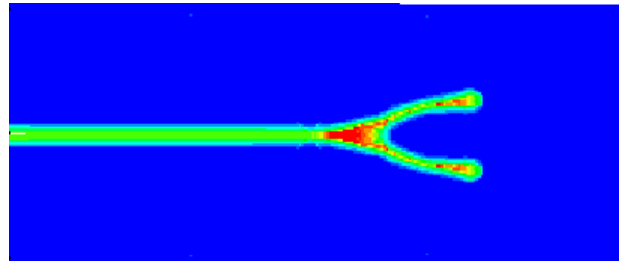
(c) m=5, Δx=0.4 mm

Figure 9: Crack propagation and brabching with different grids for δ=2 mm; the damage maps shown are at 60 μs

4.2 Verification of strength failure of brittle sandstone under uniaxial compression

Prior to the numerical study, the above PD model of the rock materials is verified by the strength failure of the sandstone induced by uniaxial compression, such as Yang et al. [Yang and Jing (2011)] had conducted. For this purpose, a rock sample similar to that Yang et al. [Yang and Jing (2011)] used in the experimental study was employed, and the material properties are shown in Tab. 2. Fig. 10 provided the geometry of the specimen. Consider a rock specimen with a pre-notch. The length of pre-notch is 2a and the crack angle (the angle between the crack and the direction of the horizontal direction) is β, respectively. For convenience and comparison, β=45° and 2a=25 mm are studied.

Table 2: Mechanical parameters of rock specimens

E (Gpa)	G(J/m^2)	ρ(kg/m^3)
28.12	30	2620
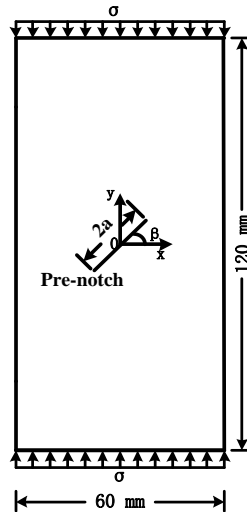
Figure 10: Specimen geometry and boundary conditions

(a)   (b)
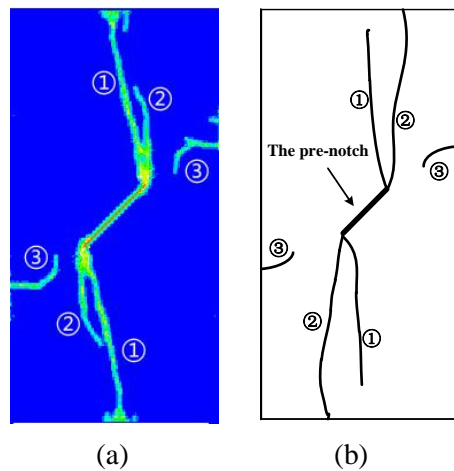
Figure 11: Comparison of the crack paths between (a) obtained from the present model and (b) from Yang et al. [Yang and Jing (2011)]

A PD model with the horizon δ=2 mm and Δx=0.5 mm is applied to the rock specimen. Fig. 11 displays the crack paths from the present model and Yang et al. [Yang and Jing (2011)] with the same condition.The results in the Fig. 11 from the PD model are very close to the experimental results by Yang et al. [Yang and Jing (2011)]. Through the above comparison,

it illustrates that the PD model for the rock material is valid and effective.

### *4.3 Double cracks in the shale material*

For shale materials, it is common that multiple cracks exists. Accordingly, it is necessary and important to study the multi-crack propagation and their interaction. In this section, we obtained a set of numerical example for shale plate under dynamic load through PD simulatioon. As we know, the shale is the bedding structure. For convenience, we consider a two-ply shale plate, which is shown in Fig. 12 [Ha, Lee and Hong (2015); Cao, Pu, Liu et al. (2015); Tang, Lin, Wong et al. (2001); Zhou, Bi and Qian (2016)]. The numerical sample with the dimensions 75 mm×150 mm and the shale plate with double cracks length of 15 mm and rock bridge length of 15 mm. β is the angle between the crack and x direction and rock bridge angle α=90°. We consider several cases for β=0°, 15°, 30°, 45°, 60°, respectively, to study the affection of β on the crack propagation. The loading condition is shown in Fig. 6 and $\sigma_0 = 11 \, \text{MPa}$. The shale material used in this study is Longmaxi Formation shale from Sichuan, China [Wang, Dong, Li et al. (2012)] and the material properties of the shale sample are shown in Tab. 3.

Table 3: Mechanical parameters of shale specimens [Wang, Dong and Li et al. (2012)]

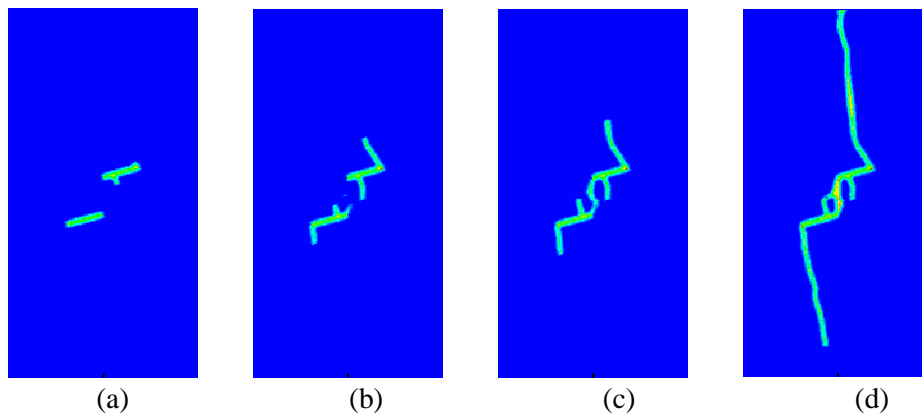| E (GPa)	K_{IC} (MPa·m$^{1/2}$)	ρ(kg/m^3)
E_1=40.84	0.99	ρ_1=2486
E_2=17.12	0.99	ρ_2=2507

(a)   (b)
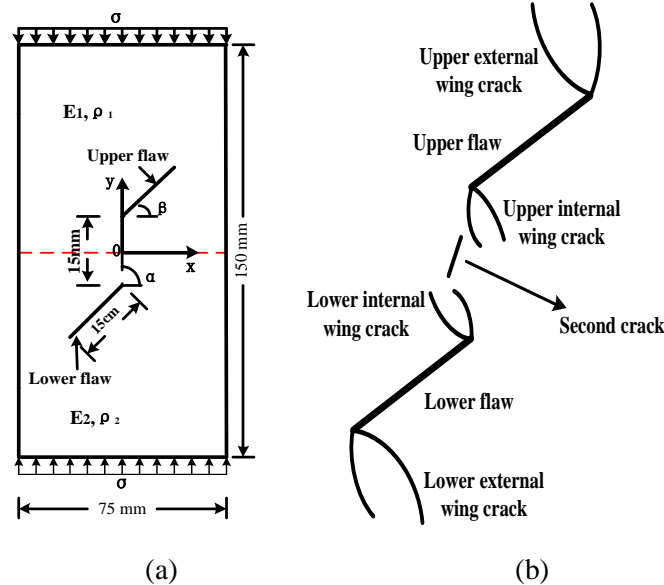
Figure 12: Shale specimen with two cracks: (a) geometry and boundary condition; (b) crack terms
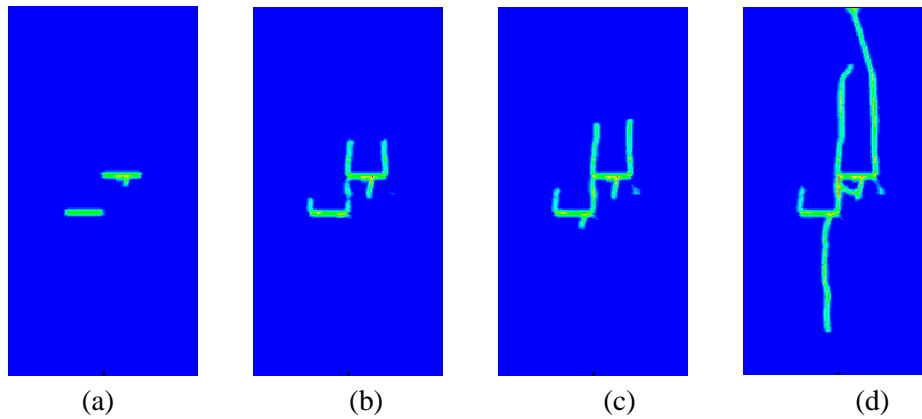
Figure 13: Snapshots of coalescence in flaw arrangements with β=0° at different instances: (a) 40 µs; (b) 54 µs; (c) 60 µs; (d) 120 µs

Figure 14: Snapshots of coalescence in flaw arrangements with β=15° at different instances: (a) 40 µs; (b) 54 µs; (c) 60 µs; (d) 120 µs
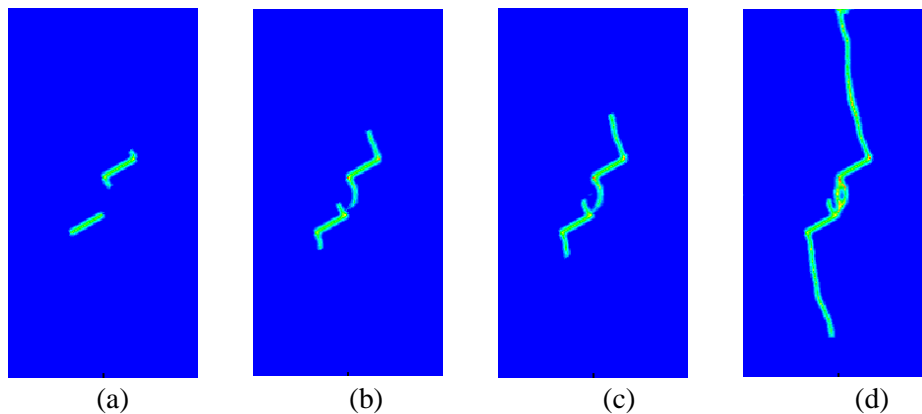
Figure 15: Snapshots of coalescence in flaw arrangements with β=30° at different instances: (a) 40 µs; (b) 54 µs; (c) 60 µs; (d) 120 µs
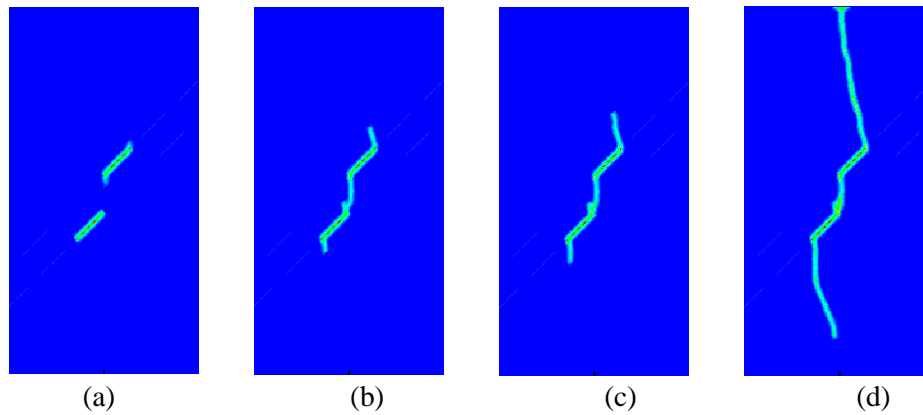
Figure 16: Snapshots of coalescence in flaw arrangements with β=45° at different instances: (a) 40 μs; (b) 54 μs; (c) 60 μs; (d) 120 μs
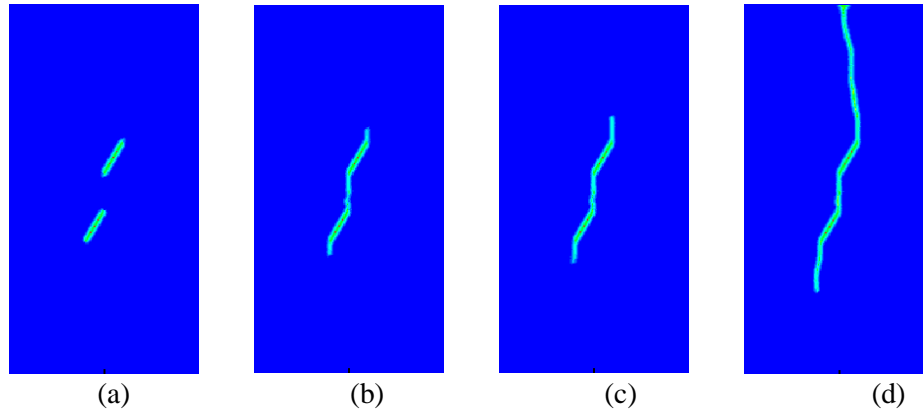
Figure 17: Snapshots of coalescence in flaw arrangements with β=60° at different instances: (a) 40 μs; (b) 54 μs; (c) 60 μs; (d) 120 μs

As can be seen from Fig. 6, the dynamic loads are suddenly applied to the boundary and remain unchanged for a subsequent period of time. This can produce stress waves in the specimen. Snapshots taken at 40 μs, 54 μs, 60 μs, 120 μs after the loads were appled for shale samples with β=0°, 15°, 30°, 45°, 60°, respectively, are presented in Figs. 13-17. It can be observed that the cracks initiation occurs at the two pre-notch tips for all the cases of β, the cracks originates from the outside tips of the cracks and propagates vertically to the top and bottom edge of the specimen, and the crack in the ply 1 propagates faster than in ply 2. Moreover, it can be found form Fig. 13 and Fig. 14 that the crack branching occurs from the inner tips of pre-crack when β=0°, 15°. Especially when β=0°, two wing cracks emanate from the tips of the pre-notchs. As β increases, the pre-existing cracks are more prone to coalesce with each other from the inner tips and propagate vertically to the top and bottom edge of the sample.

5 Conclusion

In this work, we presented a bond-based PD model for shale material with bedding structure to study its brittle dynamic fractures behavior. The dynamic crack propagation and interaction between two pre-existing cracks were discussed. We also discussed the two types of numerical convergence criteria and illustrated the the PD model is effective through the comparison with the experiment. We further studied two pre-existing cracks in shale materials with two plies subjected to dynamic uniaxial loads. The effect of the angle between the pre-notch and the horizontal direction was conducted. The numerical results indicate that the angle has a remarkable effect on the crack path and the interaction of cracks.

References

Abraham, F. (2005): Unstable crack motion is predictable. *Journal of the Mechanics and Physics of Solids*, vol. 53, pp. 1071-1078.

Agwai. A.; Guven. I.; Madenci. E. (2011): Predicting crack propagation with peridynamics: a comparative study. *International Journal of Fractcture*, vol. 171, pp. 65-78.

Belytschko, T.; Black, T. (1999): Elastic crack growth in finite elements with minimal remeshing. *International Journal for Numerical Methods in Engineering*, vol. 45, pp. 601-620.

Bobaru. F.; Yang. M.; Alves. L. F.; Silling. S. A.; Askari. E. et al. (2009): Convergence, adaptive refinement, and scaling in 1DPeridynamics. *International Journal of Numerical Methods in Engineering*, vol. 77, pp. 852-77.

Cai, M. (2013): Fracture initiation and propagation in a Brazilian disc with a plane interface: a numerical study. *Rock Mechanics and Rock Engineering*, vol. 46, pp. 289-302.

Cao, P.; Liu, T.; Pu, C.; Lin, H. (2015): Crack propagation and coalescence of brittle rock-like specimens with pre-existing cracks in compression. *Engineering Geology*, vol. 187, pp. 113-121.

Chakraborty, S.; Shaw, A. (2013): A pseudo-spring based fracture model for SPH simulation of impact dynamics. *International Journal of Impact.Engineering*, vol. 58, pp. 84-95.

Cheng, Z. Q.; Zhang, G. F.; Wang, Y. N.; Bobaru, F. (2015): A peridynamic model for dynamic fracture in functionally graded materials. *Composite Structuctures*, vol. 133, pp. 529-546.

Cheng, Z. Q.; Liu, Y. K.; Zhao, J.; Feng, H.; Wu, Y. Z. (2018): Numerical simulation of crack propagation and branching in functionally graded materials using peridynamic modeling. *Engineering Fractcure Mechanics*, vol. 191, pp. 13-32.

Fan, H. F; Li, S. F. (2017): A Peridynamics-SPH modeling and simulation of blast fragmentation of soil under buried explosive loads. *Computer Methods in Applied Mechanics and Engrgineering*, vol. 318, pp. 349-381.

Fan, H. F; Guy L. B.; Li, S. F. (2015): A Hybrid Peridynamics-SPH simulation of soil fragmentation by blast of buried explosive. *Internation Journal of Impact Engineering*, vol. 87, pp. 14-27.

Gu, X.; Zhang, Q.; Huang, D.; Yv, Y. T. (2016): Wave dispersion analysis and simulation method for concrete SHPB test in peridynamics. *Engineering Fractcure Mechanics*, vol. 160, pp. 124-137.

Ha, Y. D.; Lee, J.; Hong, J. W. (2015): Fracturing patterns of rock-like materials in compression captured with peridynamics. *Engineering Fractcure Mechanics*, vol. 144, pp. 176-193.

Ha, Y. D. ; Bobaru, F. (2011) : Characteristics of dynamic brittle fracture captured with peridynamic. *Engineering Fractcure Mechanics*, vol. 78, pp. 1156-1168.

Li, H. L.; Wong, L. N. Y. (2012): Influence of flaw inclinationangle and loading condition on crack initiation and propagation. *International Journal of Solids and Structures*, vol. 49, pp. 2482-2499.

Li, X.; Konietzky, H.; Li, X. B. (2016): Numerical study on time dependent and time independent fracturing processes for brittle rocks. *Engineering Fractcure Mechanics*, vol. 163, pp. 89-107.

Li, X. B.; Feng, D.; Li, D. Y. (2018): Numerical simulation of rock failure under static and dynamic loading by splitting test of circular ring. *Engineering Fractcure Mechanics*, vol. 188, pp. 184-201.

Lai, X.; Ren, B.; Fan, H. F.; Li, S. F.; Wu, C. T. et al. (2015): Peridynamics simulations of geomaterial fragmentation by impulse loads. *International Journal for Numerical and Analytical Methods in Geomechanics*, vol. 39, pp. 1304-1330.

Nakano, A.; Kalia, R. K.; Vashista, P. (1995): Dynamics and morphology of brittle cracks: a molecular dynamics study of silicon nitride. *Physics Review Letter*, vol. 75, pp. 3138-3141.

Ni, T.; Zhu, Q. Z.; Zhao, L. Y.; Li, P. F. (2018): Peridynamic simulation of fracture in quasi brittle solids using irregular finite element mesh. *Engineering Fractcure Mechanics*, vol. 188, pp. 320-343.

Rannou, J.; Limodin, N.; Rthore, J. (2010): Three dimensional experimental and numerical multiscale analysis of a fatigure crack. *Computer Methods in Applied Mechanics and Engrgineering*, vol. 199, pp. 1307-1325.

Raymond, S.; Lemiale, V.; Ibrahim, R.; Lau, R. (2014): A meshfree study of the Kalthoffe-Winkler experiment in 3D at room and low temperatures under dynamic loading using viscoplastic modelling. *Engineering Analysis with Boundary Elements*, vol. 42, pp. 20-25.

Ravi-Chander, K.; Knauss, W. G. (1984a): An experimental investigation into dynamic fracture: II Microstructural aspects. *International Journal of Fracture*, vol. 26, pp. 65-80.

Ravi-Chander, K.; Knauss, W. G. (1984b): An experimental investigation into dynamic

fracture: III on steady-state crack propagation and crack branching. *International Journal of Fracture*, vol. 26, pp. 141-154.

Rabczuk, T.; Ren, H. L. (2017): A peridynamics formulation for quasi-static fracture and contact in rock. *Engineering Geology*, vol. 225, pp. 42-48.

Silling, S. A. (2000): Reformulation of elasticity theory for discontinuities and long-range forces. *Journal of the Mechanics and Physics of Solids*, vol. 48, pp. 175-209.

Silling, S. A.; Askari, E. (2005): A meshfree method based on the peridynamic model of solid mechanics. *Computers & Structures*, vol. 83, pp. 1526-1535.

Silling, S. A.; Epton, M.; Weckner, O.; Xu, J.; Askari, E. (2007): Peridynamic states and constitutive modeling. *International Journal of Elasticity*, vol. 88, pp.151-184.

Smith, G.; Schlangen, E.; Flewitt, P. E. J.; Crocker, A. G.; Hodgkins A. (2016): A model to describe the fracture of porous polygranular graphite subject to neutron damage and radiolytic oxidation. *Computers, Materials & Continua*, vol. 51, no. 3, pp. 163-185

Song, J. T.; Wang, H.; Belytschko, T. (2008): A comparative study on finite element methods for dynamic fracture. *Computational Mechanics*, vol. 42, pp. 239-250.

Tang, C. A.; Lin, P.; Wong, R. H. C.; Chau, K. T. (2001): Analysis of crack coalescence in rock-like materials containing three flaws-part II: numerical approach. *International Journal of Rock Mechanics and Mining Science*, vol. 38, pp. 925-939.

Wang, E. Z.; Shrive, N. G. (1993): On the griffith criteria for brittle fracture in compression. *Engineering Fractcure Mechanics*, vol. 46, pp. 15-26.

Wang, Y. M.; Dong, D. Z.; Li, J. Z.; Wang, S. J.; Li, X. J. et al. (2012): Reservoir characteristic of shale gas in Longmaxi Formation of the Lower Silurian, Southern Sichuan. *Acta Petrolum Sinica*, vol. 33, pp. 551-561 (In Chinese).

Wang, Y. T.; Zhou, X. P.; Xu, X. (2016): Numerical simulation of propagation and coalescence of flaws in rock materials under compressive loads using the extended non-ordinary state-based peridynamics. *Engineering Fractcure Mechanics*, vol. 163, pp. 248-273.

Wang, Y. T.; Zhou, X. P.; Shou, Y. D. (2017): The modeling of crack propagation and coalescence in rocks under uniaxial compression using the conjugated bond-based peridynamics. *International Journal of Mechanical Sciences*, vol. 128-129, pp. 614-643.

Wang, Y. T.; Zhou, X. P.; Wang, Y.; Shou Y. D. (2018): A 3-D conjugated bond-pair-based peridynamic formulation for initiation and propagation of cracks in brittle solids. *International Journal of Solids and Structures*, vol. 134, pp. 89-115.

Wong, L. N. Y.; Wu, Z. J. (2014): Application of the numerical manifold method to model progressive failure in rock slopes. *Engineering Fractcure Mechanics*, vol. 119, pp. 1-20.

Xu, D. D.; Liu, Z. L.; Liu, X. M.; Zeng, Q. L.; Zhuang, Z. (2014): Modeling of dynamic crack branching by enhanced extended finite element method. *Computational Mechanics*, vol. 54, pp. 489-502.

Yang, S. Q.; Jing, H. W. (2011): Strength failure and crack coalescence behavior of brittle sandstone samples containing a single fissure under uniaxial compression.

International Journal of Fractture, vol. 168, pp. 227-250.

Yang, Y. F.; Tang, C. A.; Xia, K. W. (2012): Study on crack curving and branching mechanism in quasi-brittle materials under dynamic biaxial loading. *International Journal of Fractture*, vol. 177, pp. 53-72.

Zhou, X. P. ; Bi, J. ; Qian, Q. H. (2016): Numerical simulation of crack growth and coalscence in rock-like materials containing multiple pre-exist flaws. *Rock Mechanics and Rock Engineering*, vol. 48, pp. 1097-1114.

Zhou, X. P.; Wang, Y. T.; Qian, Q. H. (2016): Numerical simulation of crack curving and branching in brittle materials under dynamic loads using the extended non-ordinary state-based peridynamics. *European Journal of Mechanics. A/Solids*, vol. 60, pp. 277-299.

Zhang, H.; Qiao, P. Z. (2018): An extended state-based peridynamic model for damage growth prediction of bimaterial structures under thermomechanical loading. *Engineering Fractcure Mechanics*, vol. 189, pp. 81-97.

Zi, G.; Rabczuk, T.; Wall, W. (2007): Extended meshfree methods without branch enrichment for cohesive cracks. *Computational Mechanics*, vol. 40, no. 2, pp. 367-382.